Optics Letters

Broadband optoelectronic mixer for terahertz frequency-comb measurements

Jizhao Zang,[1,2,*] Jesse S. Morgan,[3] Andreas Beling,[3] and Scott B. Papp[1,2]

[1] Time and Frequency Division, National Institute of Standards and Technology, Boulder, Colorado, USA
[2] Department of Physics, University of Colorado, Boulder, Colorado, USA
[3] Department of Electrical & Computer Engineering, University of Virginia, Charlottesville, Virginia, USA
*jizhao.zang@nist.gov

Received 21 January 2025; revised 6 March 2025; accepted 19 April 2025; posted 21 April 2025; published 5 May 2025

We demonstrate ultra-broadband optoelectronic mixing of frequency combs that provides phase-coherent detection of a repetition frequency up to 500 GHz, using a high-speed modified uni-traveling carrier (MUTC) photodiode. Nonlinear photo-electron effects in the photodiode itself enable harmonic generation and down-mixing process of combs with widely different repetition frequencies. Specifically, we generate two 25 GHz frequency combs and use an optical filter to explore coherent down-mixing to the baseband of comb spectral components across microwave, millimeter-wave, and terahertz (THz) frequencies. The exceptional noise performance of the optoelectronic mixer enables the phase-coherent measurement of millimeter-wave and THz frequency combs with an Allan deviation of $10^{-13}/\tau$ for a measurement time of τ. We further investigate the dependence of conversion loss on the reverse bias voltage and photocurrent. The experimental results indicate that we can minimize the conversion loss by operating the photodiode at an optimal voltage and maximum available photocurrent. Our work provides a solution for millimeter-wave and THz frequency-comb measurements and facilitates fully stabilized frequency combs with microresonators. © 2025 Optica Publishing Group. All rights, including for text and data mining (TDM), Artificial Intelligence (AI) training, and similar technologies, are reserved.

https://doi.org/10.1364/OL.557366

Photonic integration of optical-frequency synthesizers [1] and optical-clock dividers [2], which generate laser sources with an optical frequency programmed from a microwave frequency reference and generate microwave (MW) signals from an optical clock, respectively, have the potential to revolutionize a wide range of applications from signal generation to information processing. The synthesis of optical frequencies relies on an optical-frequency comb, which consists of equally spaced modes at frequencies $\nu_n = f_{\mathrm{ceo}} + n \times f_{\mathrm{rep}}$, where f_{ceo} is the carrier–envelope offset frequency, n is the mode number, and f_{rep} is the repetition rate. Recently, this field has been further advanced by the introduction and use of microresonator-based optical-frequency combs (microcombs) [3]. Featuring compact size, flexible dispersion engineering, and low power consumption, microresonator combs offer the opportunity to realize a single-chip solution for optical-frequency metrology.

Optical-frequency synthesis and optical-clock division require fully stabilized octave-spanning microcombs [2,4]. But to date, most examples of octave span microcombs operate with high-repetition frequency in the THz range of about 100 GHz–1000 GHz, which is challenging to phase-coherently measure with respect to a microwave frequency reference. High-repetition-frequency microcombs are preferred because of lower threshold power and larger mode spacing that facilitates extension of the comb span. To measure such large f_{rep}, experiments have used a microwave rate (f_{mw}) auxiliary frequency comb [4] or electro-optic modulation [5] for downconversion. By heterodyne detection of the two combs, we can downconvert f_{rep} to an intermediate frequency (IF) signal f_{IF} since $f_{\mathrm{rep}} = N f_{\mathrm{mw}} + f_{\mathrm{IF}}$, where N is an integer. However, these types of schemes are complicated by the relative optical phase of the two combs.

We anticipate that by photodetecting frequency combs of THz and MW repetition frequency in a high-speed photodiode, nonlinear mixing of the photocurrents will directly yield an IF, taking advantage of MW harmonic generation in the photodiode. The origin of photodiode nonlinearity [6–9] is still not fully understood. Several mechanisms contribute, such as voltage and current dependence of responsivity and junction capacitance, the space charge effect, and the Franz–Keldysh effect [10–12]. Photodiode nonlinearity is conventionally considered an adverse effect since it induces unwanted mixing products. However, nonlinearity has been explored for optoelectronic mixing [8,9,13–15]. In those experiments, frequency upconversion to the V band has been demonstrated for applications in wireless communications.

Here, we draw on advances in high-speed MUTC photodiodes [16–18] to demonstrate an ultra-broadband optoelectronic mixer operating at up to 500 GHz. Our photodiode mixer induces negligible frequency noise, allowing for Allan deviation (ADEV) frequency-noise measurements at $10^{-13}/\tau$ with the THz rate combs. We experimentally investigate the dependence of the conversion loss on photodiode's bias voltage and photocurrent, showing that an optimal bias voltage and large photocurrent is beneficial to minimizing the conversion loss. Featuring compact size, low additional noise, and broad operating bandwidth, the optoelectronic mixer we report is a promising candidate for precise detection of frequency comb f_{rep} at THz frequencies.

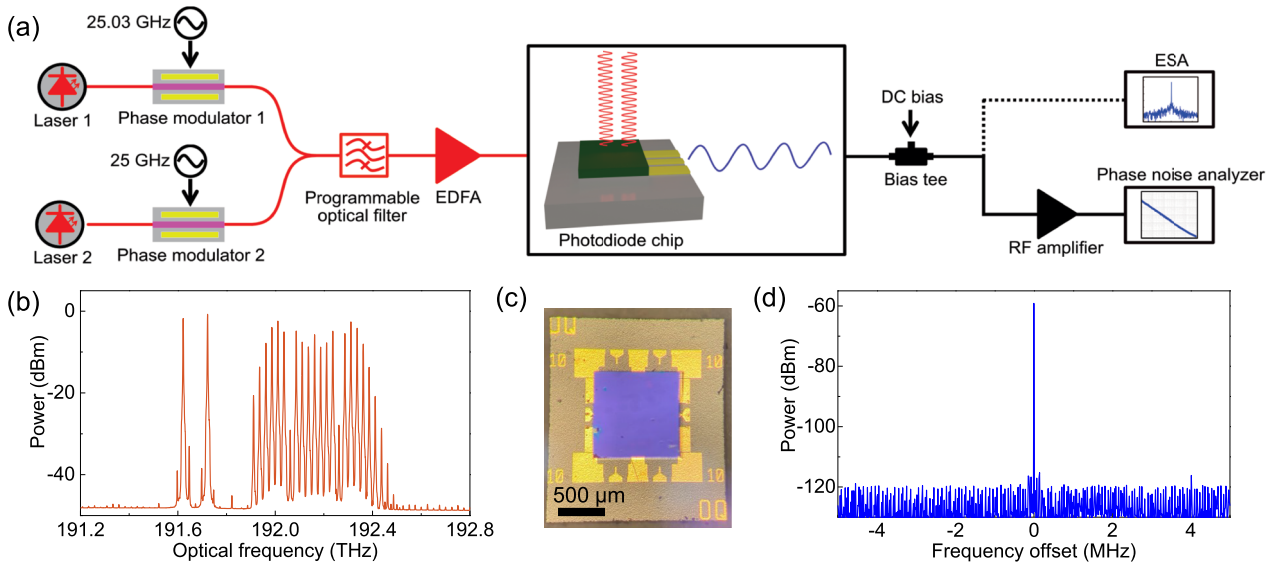

Fig. 1. Phase-coherent detection of f_{rep} using a high-speed photodiode as the optoelectronic mixer. (a) Experimental setup, including two systems of lasers and phase modulators to generate EO combs, a programmable optical filter, an EDFA, the photodiode chip, a RF amplifier, an electrical spectrum analyzer, and a phase noise analyzer. (b) Optical spectrum at the output of the EDFA, showing a 100.12 GHz millimeter-wave-rate comb and a 25 GHz microwave-rate comb. (c) Microscope image of the photodiode chip after flip-chip bonding on an aluminum nitride submount. (d) Electrical spectrum of the IF signal at 120 MHz.

Our experimental setup is shown in Fig. 1(a), including the frequency-comb generation and the optoelectronic mixer systems. We use two electro-optic (EO) frequency combs with microwave repetition frequency ($f_{mw} \approx 25$ GHz, generated by Keysight E8257D) and a programmable optical filter to generate comb spectra with widely variable harmonic repetition frequencies (f_{rep}) into the millimeter-wave and THz ranges. Operationally, we use two systems of continuous-wave (CW) lasers and phase modulators to generate two EO combs at 25.03 GHz and 25 GHz, respectively. We tune the CW lasers across the C band, so that the center frequency of the EO combs can be very different. By programming an optical filter (Finisar Waveshaper 1000S), we create combs with harmonic repetition frequencies to simulate the microcomb under test and characterize the optoelectronic mixer. We use an erbium-doped fiber amplifier (EDFA) after the filter to increase the optical power for high-nonlinearity operation of the photodiode. The output of the photodiode is connected to a bias tee, which separates the DC bias voltage and IF signal. The IF signal is either fed to an electrical spectrum analyzer (ESA) for spectrum measurement or a phase noise analyzer for ADEV measurements. Figure 1(b) shows the case of creating a 100.12 GHz millimeter-wave-rate comb from the EO comb of laser 1 and a 25 GHz microwave-rate comb from the EO comb of laser 2. For the 25 GHz microwave-rate comb, we purposely filter out some comb modes to realize phase modulation to intensity modulation conversion.

In order to maximize the power of the photo-generated electrical signal and IF signal, we design the photodiode with ultra-wide bandwidth and high power handling capability. We use a MUTC structure [16,17,19] to increase the transit-time-limited bandwidth and saturation power. To minimize the junction capacitance for high-speed operation, we reduce the active area to 5 μm in diameter. Figure 1(c) presents a microscope image of our photodiode with a 3 dB bandwidth of 128 GHz and a maximum photocurrent over 30 mA. The high-speed photodiode is flip-chip bonded on an aluminum nitride submount. On the submount, there are coplanar waveguides, which are compatible with commercial ground-signal-ground probes. The geometry of the CPWs is also optimized to further enhance the photodiode bandwidth through inductive peaking [20].

Photodetection of both combs generates not only the harmonics of their repetition rates but also their inter-modulation products because of photodiode nonlinearity. In Fig. 1(d), we present the IF signal when the photodiode is illuminated with the optical spectrum of Fig. 1(b). Here, the central frequency is $f_{IF} = f_{rep} - 4f_{mW} = 120$ MHz, where f_{rep} (100.12 GHz) is the beat note of the EO comb from laser 1 and $4f_{mw}$ (100 GHz) is generated inside the photodetector by a combination of photocurrent harmonics and the intrinsic comb tones that lead to $4f_{mw}$ in the EO comb from laser 2. Unlike the work demonstrated in [21], we employ the nonlinearity of an ultrafast photodiode and harmonics of a known microwave frequency to detect f_{rep} at hundreds of GHz. One feature of our optoelectronic mixer is that no high-frequency components are required for THz detection. The proposed mixer primarily relies on the first-order nonlinearity, with minimal contribution from higher-order nonlinearities. By operating the photodiode with large photocurrent, we can reduce the conversion loss to below 35 dB.

We investigate the noise performance of the optoelectronic mixer in the millimeter-wave frequency range by operating it to measure the repetition frequency fluctuations of two, ≈100 GHz combs. Figure 2(a) shows how we generate the 100 GHz combs by programming the optical filter to transmit only two modes from each EO comb; the gray (red) trace shows the unfiltered (filtered) EO combs measured at the EDFA output. The resulting combs have spacings of 100 GHz and 100.12 GHz, leading to an IF signal of 120 MHz; see Fig. 2(b). The IF signal has a signal-to-noise ratio (SNR) over 60 dB, making high coherence phase and frequency-noise analysis readily feasible. We measure the ADEV of the IF signal, using a conventional

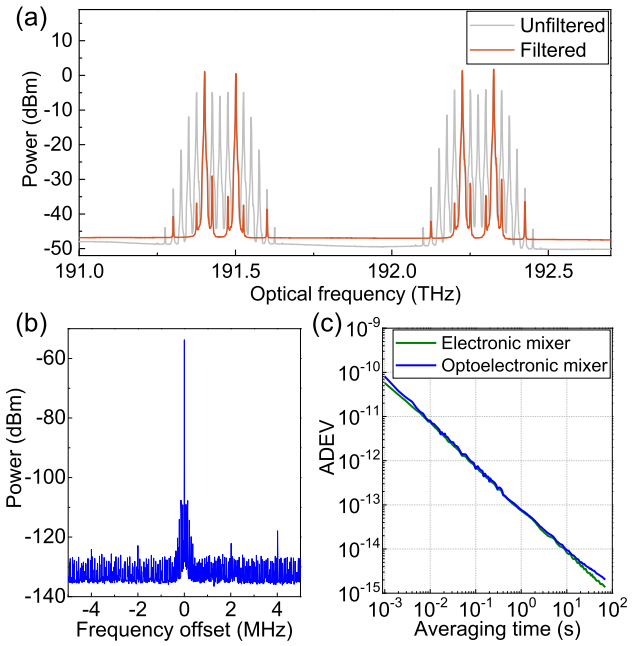

Fig. 2. Comparison of the noise performance between a conventional electronic mixer and our optoelectronic mixer. (a) Optical spectra of the unfiltered (gray) and filtered (red) EO combs. (b) Electrical spectrum of the IF signal at 120 MHz. (c) Comparison of the ADEV measured with a conventional electronic mixer and our optoelectronic mixer.

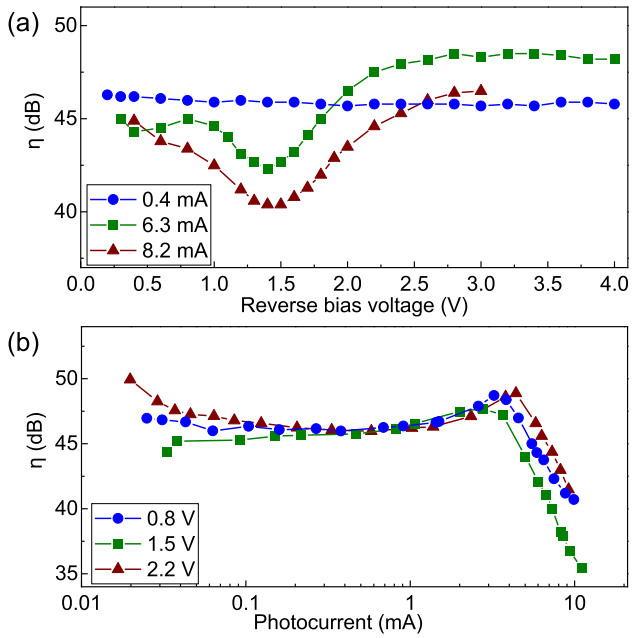

Fig. 3. Conversion loss of the optoelectronic mixer in the case of two, ≈100 GHz combs. (a) Measured conversion loss as a function of reverse bias voltage. (b) Measured conversion loss with varied photocurrent.

phase noise analyzer with the same clock input as we use to generate the 25 GHz signal for the EO combs. Hence, the ADEV of the IF signal is traceable to that of the shared clock input, providing the baseline for characterizing the noise performance. We compare the optoelectronic mixer with a conventional electronic mixer by measuring the ADEV of the IF signal in both cases; see Fig. 2(c). In the case with the electronic mixer, 25 GHz and 25.03 GHz signals used for the EO combs are fed into an electronic mixer to generate the IF signal, which allows us to estimate the fundamental noise in down-mixing of 100 GHz combs. Figure 2(c) shows that the ADEV measured with the optoelectronic mixer agrees with that measured by a conventional electronic mixer, reaching 7.7×10^{-14} at 1 s averaging time. These results indicate that the noise induced by our optoelectronic mixer is negligible compared with the conventional electronic mixer, and we observe similar noise performance at different photocurrent levels.

Photodiode nonlinearity is essential for our optoelectronic mixer, and we optimize the photodiode nonlinearity by investigating the conversion loss, which is defined as $\eta = 10\log_{10}(P_{\mathrm{mmW}}/P_{\mathrm{IF}})$, where P_{mmW} and P_{IF} are the power of the generated millimeter-wave signal and IF signal, respectively [14]. We calculate P_{mmW} at different photocurrent based on the measured P_{mmW} at 5 mA with a commercial powermeter working up to 1 THz (VDI PM5). For example, we measure η in the case of two, ≈100 GHz combs. Since both photodiode's bias voltage and photocurrent can influence its nonlinearity, we investigate η by varying one parameter while keeping the other fixed.

Figure 3(a) shows η as a function of reverse bias voltage at different photocurrent. Since P_{mmW} is nearly fixed for each photocurrent value, P_{IF} is inversely proportional to η and varies strongly with reverse bias voltage. At 0.4 mA photocurrent (blue circles), η is independent of photodiode's bias voltage. At larger photocurrent (green squares and brown triangles), η first decreases and then increases with bias voltage, resulting in a minimum η at a reverse bias voltage of 1.4 V. This trend can be explained by the competition between higher responsivity and stronger internal electric field as the reverse bias voltage increases. It is believed that the photodiode nonlinearity is related to the accumulation of photo-generated carriers in the depletion region of the photodiode (space charge). Due to the recombination of carriers, the responsivity at 0 V is lower compared with that at higher voltages. The responsivity increases with the reverse bias voltage, leading to more space charge and higher nonlinearity. This effect is dominant at reverse bias voltages below 1.4 V. Above 1.4 V, another effect becomes dominant: the strong internal electric field sweeps out the space charge and reduces the photodiode nonlinearity. For the MUTC photodiode we use, the competition between these two effects results in a minimum η at 1.4 V.

Figure 3(b) illustrates how η varies with increasing photocurrent, showing a trend of initially increasing slightly and then decreasing sharply. This trend is explained by the space charge effect. The MUTC photodiode contains an un-depleted absorption region where the movement of photo-generated electrons is mainly based on diffusion at low photocurrent level. As the photocurrent increases, an electric field, which is called self-induced field, arises in that region [22,23]. It is beneficial to electrons' transport and leads to reduced space charge and lower nonlinearity. However, this electric field is relatively weak, and the above-mentioned effect only dominates at low photocurrent level. At larger photocurrent, the accumulation of photo-generated carriers becomes the predominant effect, and the photodiode nonlinearity is enhanced by the increased space charge. These experimental results suggest that we can operate the photodiode at the saturation state to improve its nonlinearity.

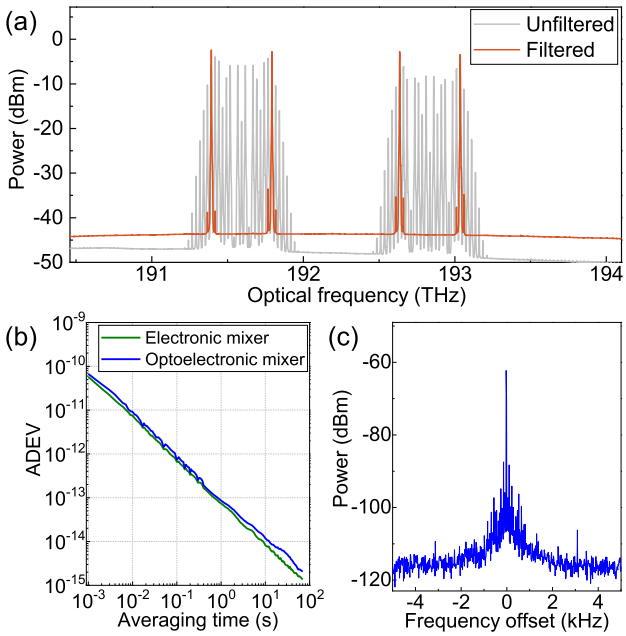

Fig. 4. Broadband frequency-noise performance of the optoelectronic mixer. (a) Optical spectrum (red) of two ≈400 GHz combs. The gray trace represents the case of unfiltered EO combs. (b) Comparison of the ADEV measured by a conventional electronic mixer and our optoelectronic mixer. (c) Electrical spectrum of the IF signal in the case with two ≈500 GHz combs.

However, we still keep the photocurrent below 11 mA to avoid thermal failure of the photodiode.

We further investigate the broadband frequency-noise performance of our optoelectronic mixer by operating it with two, ≈400 GHz combs (Figs. 4(a) and 4(b)) and two, ≈500 GHz combs (Fig. 4(c)). We use the same setup as that in Fig. 1(a), except with a higher RF power of the 25 GHz signals. Figure 4(a) shows the optical spectra in the case with (red) and without (gray) applying the multiple passband filter. By programming the optical filter, we achieve two combs with spacing of 400.12 GHz and 400 GHz, respectively. Photodetection of these two combs and down-mixing of the corresponding electrical signals yield f_{IF} at 120 MHz. Figure 4(b) shows a comparison of the ADEV between the case with the conventional electronic mixer and our optoelectronic mixer. In both cases, the ADEV is less than 8.6×10^{-14} at 1 s averaging time. The IF signal generated by our optoelectronic mixer shows slightly higher frequency noise, which results from the noise induced by optical and electrical amplifiers in the system. We further operate the optoelectronic mixer with two, ≈500 GHz combs; see Fig. 4(c). The SNR of the IF signal is low, partly due to the weak comb lines and low-SNR optical signals after the EDFA. We can improve the SNR of the IF signal by using cascaded modulators to generate 500 GHz combs with higher comb line power. Compared with the conventional electronic mixer, our optoelectronic mixer can operate over a much broader frequency bandwidth, supporting down-mixing of combs at millimeter-wave and THz ranges.

In summary, we demonstrate a broadband optoelectronic mixer, based on a high-speed MUTC photodiode. Using a single photodiode, we demonstrate phase-coherent detection of f_{rep} up to 500 GHz. The exceptional noise performance of the optoelectronic mixer is confirmed by the comparison with a conventional electronic mixer. We optimize the photodiode nonlinearity by investigating the dependence of conversion loss on photodiode's bias voltage and photocurrent. Our setup not only is an ultrafast photodiode that functions as a wideband mixer but also provides a simple and reliable method of measuring microcomb repetition frequency with a frequency comb at the microwave rate. Our work will benefit applications in optical-frequency synthesis by providing a compact and broadband solution for detection of millimeter-wave and THz repetition rates.

Funding. Air Force Office of Scientific Research (FA9550-20-1-0004 Project Number 19RT1019); Defense Advanced Research Projects Agency (A-PhI FA9453-19-C-0029); NSF Quantum Leap Challenge Institute Award (OMA – 2016244); National Institute of Standards and Technology.

Acknowledgment. We acknowledge Madison Woodson and Steven Estrella from Freedom Photonics for MUTC PD fabrication. We thank Haixin Liu and Nitesh Chauhan for the technical review of the Letter. Tradenames provide information only and not an endorsement.

Disclosures. The authors declare no conflicts of interest.

Data availability. Data underlying the results presented in this Letter are not publicly available but may be obtained from the authors upon reasonable request.

REFERENCES

1. D. T. Spencer, T. Drake, T. C. Briles, *et al.*, Nature **557**, 81 (2018).
2. T. E. Drake, T. C. Briles, J. R. Stone, *et al.*, Phys. Rev. X **9**, 031023 (2019).
3. Y. Sun, J. Wu, M. Tan, *et al.*, Adv. Opt. Photonics **15**, 86 (2023).
4. T. C. Briles, J. R. Stone, T. E. Drake, *et al.*, Opt. Lett. **43**, 2933 (2018).
5. J. R. Stone, T. C. Briles, T. E. Drake, *et al.*, Phys. Rev. Lett. **121**, 063902 (2018).
6. R. Esman and K. Williams, IEEE Photonics Technol. Lett. **2**, 502 (1990).
7. K. Williams, L. Nichols, and R. Esman, J. Lightwave Technol. **16**, 192 (1998).
8. M. Tsuchiya and T. Hoshida, IEEE Trans. Microwave Theory Tech. **47**, 1342 (1999).
9. H. Fushimi, T. Furuta, T. Ishibashi, *et al.*, Jpn. J. Appl. Phys. **43**, L966 (2004).
10. A. Beling, H. Pan, H. Chen, *et al.*, J. Lightwave Technol. **26**, 2373 (2008).
11. H. Pan, Z. Li, A. Beling, *et al.*, J. Lightwave Technol. **28**, 1316 (2010).
12. Y. Fu, H. Pan, Z. Li, *et al.*, IEEE J. Quantum Electron. **47**, 1312 (2011).
13. T. Hoshida and M. Tsuchiya, IEEE Photonics Technol. Lett. **10**, 860 (1998).
14. F.-M. Kuo, Y.-S. Wu, and J.-W. Shi, IEEE Electron Device Lett. **30**, 21 (2009).
15. H. Pan, Z. Li, and J. C. Campbell, J. Lightwave Technol. **28**, 1184 (2010).
16. Q. Li, K. Li, Y. Fu, *et al.*, J. Lightwave Technol. **34**, 2139 (2016).
17. J. S. Morgan, K. Sun, Q. Li, *et al.*, in *2018 IEEE Photonics Conference (IPC)* (2018).
18. J. S. Morgan, F. Tabatabaei, T. Fatema, *et al.*, J. Lightwave Technol. **41**, 7092 (2023).
19. C. Wei, Y. Yu, Z. Wang, *et al.*, Light: Adv. Manuf. **4**, 263 (2023).
20. M. Gould, T. Baehr-Jones, R. Ding, *et al.*, Opt. Express **20**, 7101 (2012).
21. X. Xu, J. Wu, M. Tan, *et al.*, J. Lightwave Technol. **38**, 332 (2020).
22. N. Shimizu, N. Watanabe, T. Furuta, *et al.*, Jpn J. Appl. Phys. **37**, 1424 (1998).
23. T. Ishibashi, T. Furuta, S. Kodama, *et al.*, IEICE Trans. on Electron. **E83-C**, 938 (2000).